Effects of Anionic Lipid and Ion Concentrations on the Topology and Segmental Mobility of Colicin Ia Channel Domain from Solid-State NMR†

X. L. Yao and M. Hong*

Department of Chemistry, Iowa State University, Ames, Iowa 50011

Received August 2, 2005; Revised Manuscript Received November 3, 2005

ABSTRACT: Channel-forming colicins are bacterial toxins that spontaneously insert into the inner cell membrane of sensitive bacteria to form voltage-gated ion channels. It has been shown that the channel current and the conformational flexibility of colicin E1 channel domain depend on the membrane surface potential, which is regulated by the anionic lipid content and the ion concentration. To better understand the dependence of colicin structure and dynamics on the membrane surface potential, we have used solid-state NMR to investigate the topology and segmental motion of the closed state of colicin Ia channel-forming domain in membranes of different anionic lipid contents and ion concentrations. Colicin Ia channel domain was reconstituted into membranes with different POPG and KCl concentrations. ^{1}H spin diffusion experiments indicate that the protein contains a small domain that inserts into the hydrophobic center of the 70% anionic membrane, similar to when it binds to the 25% anionic membrane. Measurements of C−H and N−H dipolar couplings indicate that, on the sub-microsecond time scale, the protein has the least segmental mobility under the high-salt and low-anionic lipid condition, which has the most physiological membrane surface potential. Measurement of millisecond time scale motions yielded similar results. These suggest that optimal channel activity requires the protein to have sufficient segmental rigidity so that entire helices can undergo cooperative conformational motions that are required for translocating the channel-forming helices across the lipid bilayer upon voltage activation.

Colicin Ia is one of the protein toxins produced by *Escherichia coli* to kill other bacteria by forming voltage-gated ion channels in the inner membrane of the target cell (*1*). The crystal structure of the soluble form shows that colicin Ia has three domains with distinct functions (*2*). The receptor-binding domain binds to the outer membrane of the target cell; the translocation domain moves the channel-forming domain across the periplasmic space to the inner membrane where it binds. The channel-forming domain of colicin Ia consists of 10 α helices. Helices 8 and 9 are entirely hydrophobic, while the rest are amphipathic and rich in basic residues. After membrane binding and prior to channel opening, the two hydrophobic helices insert into the lipid bilayer while the rest of the protein remains at the membrane−water interface (*3*). Upon voltage activation, some of the surface-bound helices cross the membrane, forming an ion-conducting channel (*4*, *5*).

Electrostatic interaction between the protein and lipids plays an important role in regulating colicin function. Previous studies showed that the initial binding of colicin to the membrane requires acidic pH and negatively charged lipids (*1*, *6*). The low pH renders the protein positively charged and thus enhances the electrostatic attraction to the anionic membrane surface. Recently, Cramer and co-workers showed that the channel activity of colicin E1, a member of the channel-forming colicin family, is affected by both the membrane surface charge density and bulk ion concentration (*7*). At different ion concentrations, the optimal channel activity requires different anionic lipid contents. Using the Gouy−Chapman theory (*8*), which describes the dependence of the membrane surface potential (ψ_0) on the surface charge density (σ) and the bulk ion concentration (c) as $F\psi_0/2RT = (8\epsilon_0\epsilon RTc)^{-1/2}\sigma$, these workers concluded that the optimal channel current occurs around a ψ_0 of −60 mV. The authors also studied the thermal flexibility of colicin E1 bound to DOPC/DOPG membranes containing 30 and 70% DOPG by measuring inter-residue distances as a function of temperature using fluorescence resonance energy transfer (FRET). Two Trp−Cys distances in the amphiphilic region of colicin E1 were measured. No thermally induced distance change was found when the protein is bound to the 70% DOPG membrane, while inter-residue distances increased by 3−13 Å with temperature in the protein bound to the 30% DOPG membrane. Since the 30 and 70% DOPG bilayers have surface potentials of −75 and −115 mV, respectively, it was concluded that when $|\psi_0|$ is much larger than 60 mV, colicin E1 becomes more rigid due to the strong electrostatic attraction with the lipids. It was suggested that this loss of thermal flexibility of the closed state of the protein, specifically the surface-bound helices, hinders the translocation of the surface helices that is necessary for subsequent channel opening (*7*).

In this work, we use solid-state NMR to investigate how membrane surface charge density and bulk ion concentration influence the topology and the segmental mobility of colicin

† This work was supported by National Science Foundation Grant MCB-93398.

* To whom correspondence should be addressed: Department of Chemistry, Iowa State University, Ames, IA 50011. Telephone: (515) 294-3521. Fax: (515) 294-0105. E-mail: mhong@iastate.edu.

10.1021/bi051540h CCC: $33.50
Published on Web 12/09/2005

Ia channel domain in the closed state. We address two questions. First, does colicin contain a domain that inserts into the center of a highly anionic membrane, or is the insertion prevented or reduced by electrostatic attraction with the lipid headgroups at the membrane surface? Second, we examine how colicin Ia channel domain changes its segmental mobility as a function of the membrane surface charge and ion concentration. Two bilayer compositions, with POPC:POPG[1] ratios of 3:1 and 3:7, and two bulk KCl concentrations, 0.03 and 0.3 M, were used to prepare the protein/lipid mixtures. Thus, a total of four different membrane surface potentials were examined. We use a two-dimensional (2D) ^{1}H spin diffusion experiment (*3*) to determine the topology of the protein, and use dipolar couplings and exchange NMR to examine the segmental mobility of the protein on the sub-microsecond and millisecond time scales. We find that the side chain and backbone mobility of the protein is reduced rather than increased at the most physiological membrane surface potential, suggesting that local residue rigidity is important for large-scale conformational rearrangements of the protein.

MATERIALS AND METHODS

Protein Expression. 1-Palmitoyl-2-oleoyl-*sn*-glycero-3-phosphocholine (POPC) and 1-palmitoyl-2-oleoyl-*sn*-glycero-3-phosphoglycerol (POPG) were purchased from Avanti Polar Lipids, Inc. (Alabaster, AL), and used without further purification. $^{15}NH_4Cl$, [^{15}N]Glu, [^{15}N]Gln, and [1,6-^{13}C]-glucose were purchased from Cambridge Isotope Laboratories (Andover, MA). Unlabeled amino acids were purchased from Sigma (St. Louis, MO).

Colicin Ia channel domain with an amino-terminal His_6 tag was expressed from pKSJ120-containing *E. coli* BL21 cells and purified on His-Bind metal chelation resin as described previously (*9*). The protein was labeled selectively and extensively with ^{13}C and uniformly with ^{15}N following the TEASE protocol (*10*). [1,6-^{13}C]Glucose was used as the sole carbon source in the minimal medium. This resulted in ^{13}C labeling of Ala β, Leu α, δ1, δ2, Ser β, Val γ1, γ2, His δ2, Phe β, γ, δ1, δ2, Tyr β, δ1, δ2, ζ, and Trp β, δ1, δ2 (*10*, *11*). These residues were also labeled with ^{15}N. Only the aliphatic ^{13}C signals of the protein were analyzed in the spectra, since the aromatic and carbonyl ^{13}C signals of the protein have low sensitivities and partially overlap with the natural abundance lipid signals.

NMR Sample Preparation. To prepare membrane-bound colicin Ia channel domain, we codissolved POPC and POPG lipids in chloroform, and then evaporated the solvent under a stream of nitrogen gas. The resulting lipid film was dissolved in cyclohexane, frozen in liquid nitrogen, and freeze-dried under a vacuum of ~50 μbar. Approximately 25 mg of the dried lipid powder was dissolved in 1 mL of buffer solution containing 10 mM KCl and 10 mM citrate (pH 4.8). The lipid suspension was vortexed and freeze-thawed five times (*12*), and then extruded across polycarbonate filter membranes (5 times across the 200 nm filter and 11 times across the 100 nm filter) to produce large unilamellar vesicles (*13*). Aliquots of the extruded vesicle solution were combined with the appropriate volume of the protein solution to reach a final P:L molar ratio of 1:100. The mixture was then ultracentrifuged at 150000*g* for 2 h using a Beckman SW60 Ti rotor. The supernatant was analyzed by a photometric protein assay for the unbound protein (*14*). For the 25% POPG sample with 0.03 M KCl, only 5% of the protein remained in the supernatant, while for the 70% POPG sample with 0.03 M KCl, no protein was detected in the supernatant. The mass of water in the wet pellet is ~1.5 times that of the dry powder. To remove excess water, the membrane pellet was lyophilized and rehydrated to 35% water by mass. This process increased the final KCl concentration from 0.01 to 0.03 M. The lyophilization step does not cause protein aggregation, as shown by the presence of clear spin diffusion cross-peaks between the lipid acyl chain ^{1}H signals and the protein ^{13}C resonances (Figure 2), which indicate that the protein is in molecular contact with the lipids rather than being aggregated and phase-separated from the lipids. Moreover, ^{2}H spectra of chain-perdeuterated d_{31}-POPC in colicin-containing POPC/POPG membranes prepared with and without lyophilization showed the same quadrupolar couplings (spectra not shown), indicating that lyophilization does not change the protein−lipid interaction. The couplings in both spectra are significantly smaller than those of the protein-free membrane. This indicates that colicin Ia channel domain is homogeneously mixed rather than aggregated in the bilayer, which causes lateral expansion of the bilayer, which in turn increases the chain disorder and decreases the quadrupolar couplings.

To prepare the membrane-bound colicin sample with 0.3 M KCl, we mixed the protein and the lipids in a 0.1 M KCl buffer, but no pellet was obtained after ultracentrifugation. Ultracentrifugation of pure lipids under the same KCl concentration similarly gave no precipitation. Thus, at high ion concentrations, the hydrated ions bound to the membrane surface create sufficiently strong electrostatic repulsion to prevent vesicle adhesion (*15*). To solve this problem, we prepared the membrane-bound colicin under 0.01 M KCl, and then hydrated the pellet to 35% using a KCl solution with a suitable concentration to achieve a final ion concentration of 0.3 M.

The soluble colicin sample was prepared by directly transferring ~10 mg of the protein powder into a 4 mm magic-angle spinning (MAS) rotor, and then hydrated to 35% water by mass.

NMR Spectroscopy. All NMR experiments were carried out on a Bruker (Karlsruhe, Germany) DSX-400 spectrometer operating at a resonance frequency of 100.71 MHz for ^{13}C, 400.49 MHz for ^{1}H, and 40.59 MHz for ^{15}N. A triple-resonance MAS probe with a 4 mm spinning module was used. The ^{1}H radio frequency (rf) field strengths for heteronuclear TPPM decoupling (*16*) were 70 kHz. ^{1}H and ^{13}C 90° pulse lengths were typically 3.5 and 5.0 μs, respectively. The cross polarization (CP) contact time varied between 0.3 and 0.7 ms. Spinning speeds were regulated to ±2 Hz by a pneumatic control unit. Recycle delays of 2−3 s were used. All experiments were carried out at room temperature ($T = 293 \pm 1$ K).

A 2D ^{13}C-detected ^{1}H spin diffusion experiment was used to probe the depth of insertion of colicin Ia channel domain

[1] Abbreviations: POPC, 1-palmitoyl-2-oleoyl-*sn*-glycero-3-phosphatidylcholine; POPG, 1-palmitoyl-2-oleoyl-*sn*-glycero-3-phosphatidylglycerol; DIPSHIFT, dipolar shift correlation; LG-CP, Lee−Goldburg cross polarization; CODEX, centerband only detection of exchange; CSA, chemical shift anisotropy.

in the membrane (*3*). The ^{1}H magnetization of the mobile lipid and water is selected by a 1 ms T_2 filter and evolves under the chemical shift interaction during the t_1 period. A 90° pulse stores this ^{1}H magnetization along the *z*-axis for a mixing time t_m, during which spin diffusion occurs. Mixing times of 9−729 ms were used. The lipid ^{1}H magnetization transferred to the protein is detected through the protein ^{13}C signals after a short (300 μs) ^{1}H−^{13}C CP step. Cross-peaks in the 2D spectra were integrated, corrected for ^{1}H T_1 relaxation, and plotted as a function of $\sqrt{t_m}$ to give the spin diffusion buildup curves, from which the lipid−protein distances is obtained (*3*).

A ^{15}N CODEX experiment was used to measure slow molecular reorientations (*17*, *18*). The ^{15}N CSA is recoupled by two 180° pulses per rotor period for *n* rotor periods. The magnetization is stored along *z* for a period t_m. Then an identical CSA recoupling period refocuses the CSA evolution. If no slow reorientation occurs during t_m, then the CSA evolution is completely refocused and a full echo is observed. If molecular reorientation occurs, the CSA refocusing is incomplete, thus reducing the echo intensity. Since the protein is labeled with ^{13}C, the ^{15}N 180° pulses also recouple the ^{13}C−^{15}N dipolar couplings. Thus, a ^{13}C 180° pulse is applied in the middle of the ^{15}N CSA recoupling period to remove the ^{13}C−^{15}N dipolar couplings. To correct for ^{15}N T_1 relaxation during t_m, a short *z* filter t_z is inserted before detection. For every mixing time, a control spectrum (S_0) was measured by interchanging t_m and t_z. The relaxation-free exchange intensity is obtained as S/S_0. The mixing time was varied from 10 to 350 ms. The ^{15}N 180° pulse was 10 μs. The total CSA recoupling period was 0.6 ms. The experiments were performed at a spinning speed of 10 kHz.

C−H and N−H dipolar couplings were measured using a dipolar shift correlation (DIPSHIFT) experiment (*19*). After CP from ^{1}H, a MREV-8 pulse train was applied on the ^{1}H channel to decouple the homonuclear interaction (*20*). The X magnetization (X = ^{13}C or ^{15}N) evolves under the ^{1}H−X dipolar couplings. The duration of the MREV-8 period was incremented within one rotor period (τ_r) to constitute the t_1 period. An X 180° pulse at the end of the first rotor period and an additional τ_r refocus the X isotropic shift evolution. The ^{1}H−X dipolar coupling was extracted from the time oscillation of the X magnetization as a function of t_1. A spinning speed of 3401 Hz was used. Six MREV-8 cycles were fit into one rotor period, with a ^{1}H 90° pulse of 3.4 μs. The reported X−^{1}H couplings in Table 3 were corrected for the MREV-8 scaling factor of 0.47 (*20*).

One-bond N−H dipolar couplings were also measured using the 2D LG-CP experiment (*21*, *22*). This experiment recouples the N−H dipolar interaction under fast MAS by satisfying the sideband matching condition during CP. The CP contact time was incremented as t_1. ^{1}H spin diffusion is suppressed by spin-locking the ^{1}H magnetization along the magic angle in the spin space. The experiment was carried out at a spinning speed of 8 kHz, with a maximum t_1 of 1.5 ms, satisfying the first-order sideband condition $\omega_{1N} = \omega_{eff,H} - \omega_r$.

RESULTS

Depth of Insertion of Colicin Ia Channel Domain. Figure 1 shows the ^{13}C CP-MAS spectra of the POPC/POPG (3:7) membrane, the lipid-free soluble colicin, and the membrane-bound colicin. The amino acid type assignment is indicated in panel c.

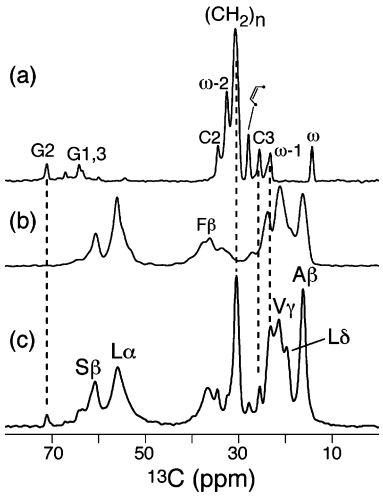

FIGURE 1: ^{13}C CP-MAS spectra of (a) the POPC/POPG membrane (3:7 molar ratio), (b) soluble colicin Ia channel domain, and (c) colicin Ia channel domain bound to the 70% POPG membrane with 0.03 M KCl. Residue-type assignments are given in panel c.

The 2D ^{1}H−^{13}C correlation experiment with ^{1}H spin diffusion is used to measure the depth of insertion of colicin in lipid bilayers (*3*, *23*). By monitoring the time-dependent increase in protein ^{13}C intensities after spin diffusion from the lipids, we obtain semiquantitative information about the proximity between lipid functional groups at various depths of the bilayer and the protein. Our earlier ^{1}H spin diffusion experiments on colicin bound to 3:1 POPC/POPG bilayers indicated that a small portion of the protein inserts into the membrane center, supporting the "umbrella" model (*24*). To investigate whether higher levels of anionic lipids prevent insertion and keep the protein on the membrane surface, we now carried out the 2D spin diffusion experiment using the 3:7 POPC/POPG membranes with 0.03 M KCl. Figure 2a shows a representative 2D spectrum, recorded with a short spin diffusion mixing time of 49 ms. Clear cross-peaks between the lipid acyl chain protons and the protein ^{13}C signals are observed, immediately indicating that the protein contains a well-inserted domain in the hydrophobic region of the bilayer, in the proximity to the lipid chain methylene and methyl protons. The buildup curve from the lipid methyl protons to the protein is shown in Figure 2b (●). For comparison, the previously measured methyl proton buildup curve for the 25% anionic membrane sample is reproduced (△). It can be seen that the 70% POPG membrane gives slightly faster intensity buildup. Quantitative distances are obtained by simulating the buildup curve using a one-dimensional lattice model and diffusion coefficients estimated from ^{1}H−^{1}H dipolar couplings (*3*, *23*). Diffusion coefficients of 0.025 and 0.005 nm^2/ms were used for lipid−lipid and lipid−protein interfacial diffusion, respectively (Table 1). These are approximately twice the values used for the 25% POPG sample, and were necessary for reproducing the shape of the buildup curve. As before, the diffusion coefficient of the protein is much higher, 0.3 nm^2/ms, due to the relative rigidity of the protein. The thickness of the source methyl groups along the bilayer normal is ∼0.6 nm (*2*), while the length of the polypeptide chain is 15 nm (*3*, *25*). Using these

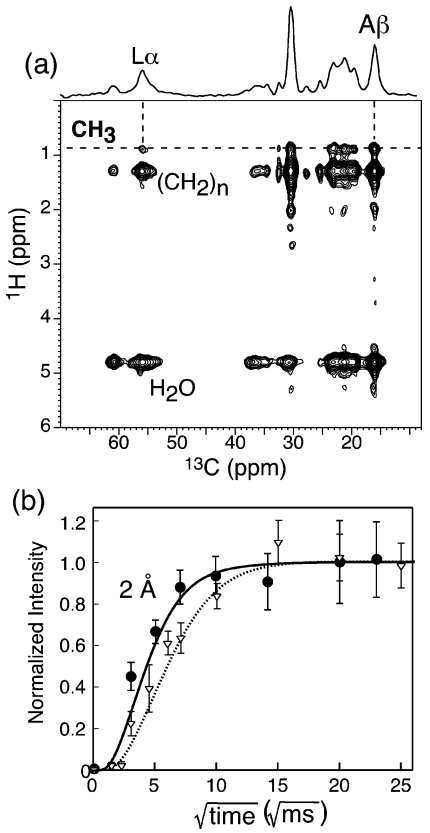

FIGURE 2: (a) Representative 2D $^{13}C-^{1}H$ correlation spectrum of colicin Ia channel domain bound to the 70% POPG membrane with 0.03 M KCl. The mixing time was 49 ms. The cross-peak between Aβ and lipid CH_3 is analyzed. (b) Methyl proton buildup curve for the 70% POPG membrane (●) and the 25% POPG membrane (▽), the latter reproduced from ref *3* for comparison. The solid line is the best fit for the 70% POPG colicin data using a 2 Å methyl−protein distance. The dotted line is the best fit for the 25% POPG colicin curve with a 2 Å distance but smaller diffusion coefficients (see the text).

Table 1: Diffusion Coefficients (D) and Thicknesses Used in ^{1}H Spin Diffusion Simulations for Colicin Ia Channel Domain Bound to the 70% POPG and 0.03 M KCl Membrane

	D (nm^2/ms)	thickness (nm)
lipid source	0.025	0.6
P−L interface	0.005	0.2
protein	0.3	15

parameters, we find a best-fit lipid−protein distance of 2 Å for the methyl proton buildup curve.

Slow Molecular Reorientations. To examine motions on the millisecond to second time scales, we carried out ^{15}N CODEX experiments on soluble and membrane-bound colicins. The motional correlation time (τ_c) is extracted by fitting the magnetization decay as a function of mixing time (t_m) using a single exponential with a constant offset ($S/S_0 = a + be^{-t_m/\tau_c}$). The constant a reflects the nonmoving fraction of colicin. The results are shown in Figure 3. The soluble colicin exhibits a long τ_c of 308 ms and a high equilibrium value of 0.9 (dashed curves), indicating a lack of slow motion. For the 25% POPG-bound colicin samples at two KCl concentrations (Figure 3b), the sample with the higher KCl concentration has a larger immobilized fraction, but the correlation time τ_c is comparable between the two (Table 2). In comparison, the 70% POPG-bound colicin (Figure 3a) samples exhibit comparable immobile fractions

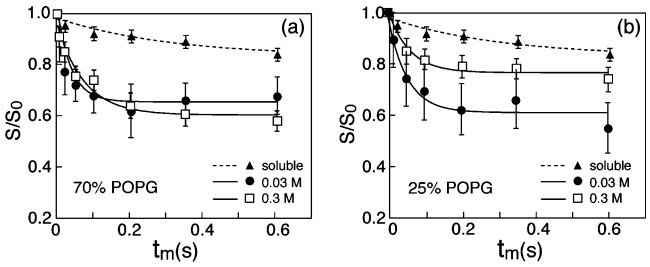

FIGURE 3: Normalized ^{15}N CODEX dephasing, S/S_0, as a function of mixing time. (a) Colicin bound to the 70% POPG membrane. (b) Colicin bound to the 25% POPG membrane. In panels a and b, the data for soluble colicin are shown (▲) for comparison, along with data for (□) 0.3 M KCl and (●) 0.03 M KCl.

Table 2: CODEX Correlation Times (τ_c) and Nonmoving Fractions (a) for Colicin Ia Channel Domain Bound to Different Membranes

POPG	[KCl] (M)	τ_c (ms)	a
70%	0.03	18 ± 4.0	0.64 ± 0.14
	0.3	75 ± 20	0.60 ± 0.03
25%	0.03	52 ± 15	0.61 ± 0.02
	0.3	58 ± 16	0.77 ± 0.01

but different τ_c values: the higher ion concentration has a significantly longer motional correlation time (Table 2). Overall, the protein is the most immobilized at the high ionic strength (0.3 M KCl) and the low anionic lipid content (25% POPG).

C−H and N−H Dipolar Couplings. C−H and N−H dipolar couplings were measured by 2D correlation experiments to probe sub-microsecond motions in colicin. Panels a and b of Figure 4 show the dipolar dephasing curves of Ala Cβ. As for the slow motion results, the soluble protein (□) is the most rigid with a coupling strength of 4.8 kHz after scaling by MREV-8. With 0.03 M KCl, the membrane-bound colicin exhibits the same coupling (3.8 kHz) for both the 25 and 70% POPG membranes. At 0.3 M KCl, the coupling increases to 4.3 kHz for the 70% POPG sample and 4.8 kHz for the 25% POPG sample. Thus, high salt and low anionic lipid concentrations increase the rigidity of the membrane-bound protein. The increased rigidity under high-salt conditions is also observed for backbone sites such as Leu Cα (Figure 4c,d). The C−H coupling is 9.0 kHz at 0.03 M KCl but increases to 10.5 kHz at 0.3 M KCl for both the 25 and 70% POPG samples. Both values are weaker than the 11 kHz coupling measured for the soluble protein.

The measured C−H and N−H dipolar couplings from the DIPSHIFT experiments are summarized in Table 3. We define a reduction factor K as the ratio between the coupling of the membrane-bound protein and the coupling of the soluble protein. Low K values indicate higher mobility, while a K value of 1.0 indicates the same rigidity as the soluble protein. At the low KCl concentration of 0.03 M, the K values are almost the same between the two POPG contents: 0.70−0.80 for the side chains and ∼0.85 for the backbone. The lower K values for the side chains indicate that the increased mobility originates from the thermal motions of the lipid molecules, which have more extensive contacts with the protein side chains than with the backbone. The fact that at low ionic strength, the K values are similar between the 70 and 25% POPG samples suggests that the binding affinity of colicin for these membranes is similar. At 0.3 M KCl, the K values are larger. For the 70% POPG

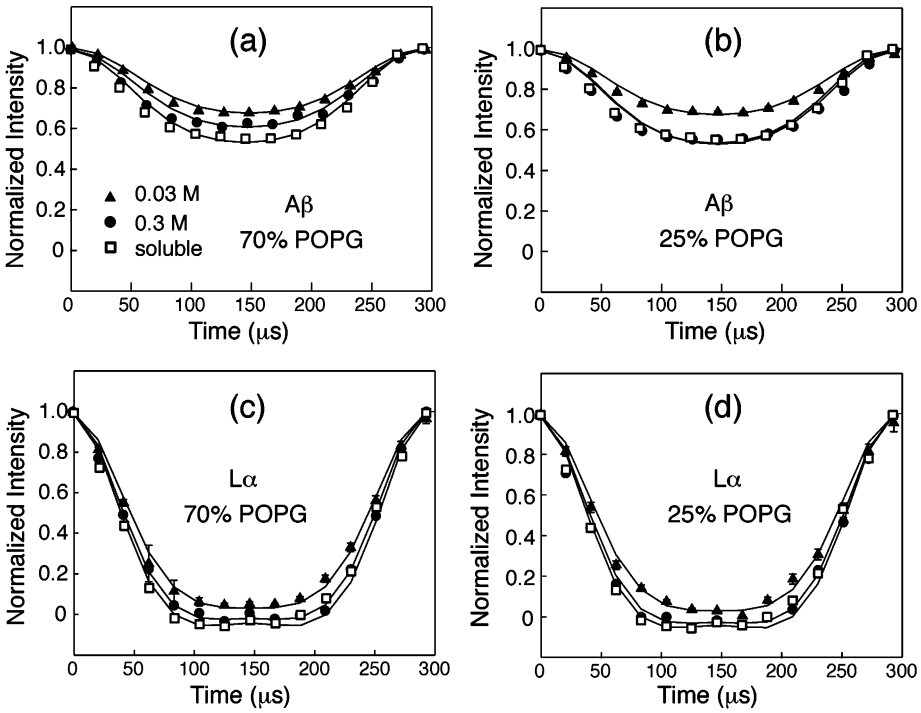

FIGURE 4: C−H dipolar couplings of selected sites in colicin Ia channel domain: (□) soluble colicin, (●) 0.3 M KCl, and (▲) 0.03 M KCl. (a) Ala Cβ, in colicin bound to the 70% POPG membrane. (b) Ala Cβ, in colicin bound to the 25% POPG membrane. (c) Leu Cα, in colicin bound to the 70% POPG membrane. (d) Leu Cα, in colicin bound to the 25% POPG membrane.

Table 3: C−H and N−H Dipolar Couplings (kilohertz) in Colicin Ia Channel Domain

		70% POPG				25% POPG				soluble
	site	0.03 M	K[a]	0.3 M	K[a]	0.03 M	K[a]	0.3 M	K[a]	colicin
N−H		9.0	0.85	9.0	0.85	9.0	0.85	9.6	0.90	10.6
C−H	Lα	19.1	0.86	21.3	0.95	19.1	0.86	21.3	0.95	22.3
	Sβ	11.9	0.70	12.8	0.75	11.7	0.69	14.9	0.88	17.0
	Aβ	8.1	0.79	9.0	0.88	8.1	0.79	10.2	1.0	10.2
	Vγ	6.8	0.76	8.1	0.91	6.4	0.72	8.5	0.95	8.9
	Lδ	6.8	0.75	8.1	0.90	6.8	0.75	8.5	0.94	9.0
⟨*K*⟩	backbone		0.85		0.90		0.86		0.93	1.0
	side chain		0.75		0.86		0.74		0.94	1.0

[a] *K* is the ratio of the couplings of the membrane-bound colicins over the soluble colicin.

sample, the *K* values of C−H bonds increase to 0.75−0.95 while there is no observable change for the N−H bonds. For the 25% POPG sample, an even larger increase in *K* is observed. The side chain *K* values are 0.94−1.0 except for that of Ser Cβ, which is 0.88 compared to 0.75 in the 70% POPG sample. The *K* of the N−H bonds increases to 0.90.

We also used the 2D LG-CP experiment to measure the N−H dipolar couplings. The soluble colicin spectrum (Figure 5d) serves as a reference with a splitting of 5.7 kHz, which is slightly smaller than the splitting of 6.2 kHz found for the crystalline model compound [^{15}N]tBoc-Gly, indicating the presence of small-amplitude motions in the soluble protein. The spectra of the membrane protein at 0.03 M KCl (Figure 5a,b) show the same outer splitting as the soluble protein but in addition have significant intensities in the center of the spectra. These suggest that the mobility of the membrane-bound colicin Ia channel domain is heterogeneous: some residues undergo much larger-amplitude motions than in the soluble state, while others are comparable to those of the soluble protein. The N−H LG-CP spectrum of the protein in the 25% anionic membrane with 0.3 M KCl

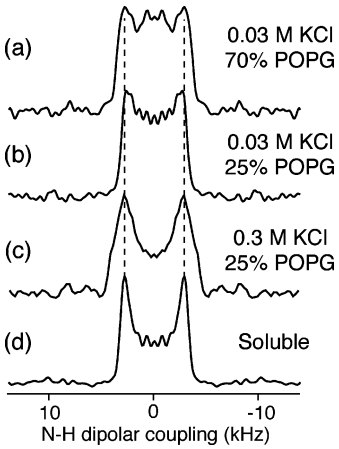

FIGURE 5: N−H dipolar spectra extracted from the 2D LG-CP spectra. (a) Colicin bound to the 70% POPG membrane with 0.03 M KCl. (b) Colicin bound to 25% POPG with 0.03 M KCl. (c) Colicin bound to 25% POPG with 0.3 M KCl. (d) Soluble colicin.

is shown in Figure 5c. Compared to the intensity of the two low-salt spectra, the intensity of the small coupling component decreased noticeably, indicating that the fraction of mobile residues decreased. Moreover, the line shape deviates from uniaxial symmetry ($\eta = 0$). Since the line shape of LG-CP spectra has been shown to depend on the asymmetry parameter, η, of the motionally averaged dipolar tensor (*22*), this suggests that under the high-salt and low-anionic lipid conditions, not only does the mobile fraction of the protein decrease but also the geometry of segmental motion changes.

DISCUSSION

To relate the NMR-determined segmental mobility and depth of insertion of colicin Ia channel domain to the membrane surface potential (ψ_0) and channel activity, we first estimate the ψ_0 values of the four membrane samples

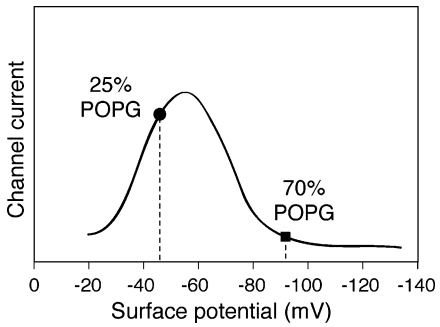

FIGURE 6: Estimated channel activities of colicin Ia channel domain bound to 25% (●) and 70% POPG (■) membranes with 0.3 M KCl. The curve is reproduced from measurements on colicin E1 (*7*).

used in our study using the Gouy−Chapman theory (*8*). The most negative ψ_0 occurs at 70% POPG under 0.03 M KCl and is approximately −146 mV. Our experiments indicate that this condition gives rise to the most dynamic form of the membrane-bound colicin on the sub-microsecond and millisecond time scales. The least negative ψ_0, approximately −46 mV, occurs at 25% POPG with 0.3 M KCl. This is the membrane potential that gives rise to the optimal channel activity in colicin E1, as illustrated in Figure 6 (*7*). In this membrane, the protein is the most rigid, as manifested by the high C−H and N−H order parameters (Table 3), which indicate small motional amplitudes, and by the large immobile fraction and long correlation times in the CODEX experiment (Table 2). The two other membrane conditions, 70% POPG with 0.3 M KCl and 25% POPG with 0.03 M KCl, have a ψ_0 of approximately −90 mV, at which colicin E1 exhibited little channel activity. These samples exhibit intermediate segmental mobility.

The main finding from this study is that among the four membrane surface potentials, the one that is closest to the physiological condition and that induces the optimal channel activity (25% POPG with 0.3 M KCl) gives rise to the most rigid protein. At first, this seems to contradict the previous conclusion that conformational flexibility is responsible for colicin channel activity, and that the reduced channel activity at more negative membrane potentials (approximately −115 mV) results from the immobilization of the surface helices (*7*). However, it is important to realize that the mobility examined previously using FRET was long-range conformational rearrangement of the protein, while the mobility investigated here using solid-state NMR is the local side chain and backbone torsional libration. The FRET experiments with colicin E1 channel domain probed interhelical distances of 25−40 Å. At the physiological membrane surface potentials of −75 mV, these distances increased by 3−13 Å due to heating, while at more negative surface potentials, the protein exhibited no thermally induced distance change. In comparison, the conformational motions probed by solid-state NMR are short-range segmental reorientations of the bonds and occur on faster time scales than the fluorescence experiments. Thus, the solid-state NMR experiments provide information that complements the fluorescence studies. The fact that colicin Ia channel domain at physiological membrane potentials shows the smallest-amplitude segmental motion suggests that for the channel to open and function properly, the amino acid residues within individual helices need to move cooperatively as rigid units, and that excessive local segmental motion is counterproductive. Conversely, in membranes with large negative potentials, the protein exhibits larger-amplitude and faster segmental motions, which inhibit the large-scale conformational change necessary for the insertion of the surface-bound helices.

Since the lipid-free soluble colicin is the most rigid state, the observed difference in mobility among the various membrane-bound states of the protein may be considered to reflect different extents of protein−lipid interactions. Stronger interactions with the lipid molecules lead to the higher segmental mobility of the protein. Since colicin Ia channel domain is positively charged at acidic pH, protein binding to the 70% anionic membranes is expected to be stronger than binding to the 25% anionic membrane; thus, the segmental motion is facilitated by the high anionic lipid content. Electrostatic interactions may also explain the increased rigidity of the protein at high ion concentrations, since ions partially screen and thus weaken the protein−lipid interactions.

The ^{1}H spin diffusion curve of the 70% POPG and 0.03 M KCl membrane rises slightly faster than that of the 25% POPG sample. This could be the result of the slightly increased rigidity of the lipids, which increases the diffusion coefficients, but could also reflect a true deeper insertion of colicin into the more anionic membrane. Kienker and coworkers found that in the closed state of colicin, the hydrophobic hairpin exists in an equilibrium between the cis and trans sides of the membrane (*4*). At pH 9.0, the helical hairpin is predominantly on the cis side, while at pH 6.0, the equilibrium is shifted more to the trans side. This suggests that the ^{1}H spin diffusion curve may reflect an average of the cis and trans states of the helical hairpin: the more dominant the trans state, the faster spin diffusion from the acyl chains to the protein. While we did not vary the pH of the samples, the anionic lipid content may very well play a similar role in regulating the insertion of the helical hairpin: the more negative charges on the membrane surface, the less favorable it is for the hydrophobic helices to remain on the surface, and the higher the probability of the trans state. This may explain the slightly faster spin diffusion buildup curve of the 70% POPG sample compared to that of the 25% POPG sample.

In summary, we determined the depth of insertion and segmental motion of the closest-state colicin Ia channel domain as a function of the ion concentration and anionic lipid content using solid-state NMR. ^{1}H spin diffusion experiments showed that the closed-state colicin has a completely inserted domain in the 70% anionic membrane, similar to when it binds to the 25% anionic membrane. Thus, the insertion of the hydrophobic helical hairpin is not hindered but rather facilitated by the anionic headgroups at the membrane surface. C−H and N−H dipolar couplings show that all membrane-bound colicins undergo larger-amplitude segmental motions than soluble colicin, but the degree of motion differs for different anionic lipid contents and ion concentrations. The most rigid protein is found at high-salt and low-anionic lipid contents, which correspond to the most physiological membrane surface potential. The same trend is observed for motions on the millisecond time scale. Thus, optimal channel activity at physiological membrane potentials requires restricted segmental motion, sug-

gesting that the proper function of the channel domain of colicins requires entire helices to move cooperatively as internally rigid units.

ACKNOWLEDGMENT

We thank Emily Seeberger and Wenbin Luo for assistance in the experiments.

REFERENCES

1. Cramer, W. A., Heymann, J. B., Schendel, S. L., Deriy, B. N., Cohen, F. S., Elkins, P. A., and Stauffacher, C. V. (1995) Structure−function of the channel-forming colicins, *Annu. Rev. Biophys. Biomol. Struct. 24*, 611−641.
2. Wiener, M., Freymann, D., Ghosh, P., Stroud, R. M. (1997) Crystal structure of colicin Ia, *Nature 385*, 461−464.
3. Huster, D., Yao, X., and Hong, M. (2002) Membrane protein topology probed by ^{1}H spin diffusion from lipids using solid-state NMR spectroscopy, *J. Am. Chem. Soc. 124*, 874−883.
4. Kienker, P. K., Qiu, X., Slatin, S. L., Finkelstein, A., and Jakes, K. S. (1997) Transmembrane insertion of the colicin Ia hydrophobic hairpin, *J. Membr. Biol. 157*, 27−37.
5. Qiu, X., Jakes, K. S., Kienker, P. K., Finkelstein, A., and Slatin, S. L. (1996) Major transmembrane movement associated with colicin Ia channel gating, *J. Gen. Physiol. 107*, 313−328.
6. Mel, S. F., and Stroud, R. M. (1993) Colicin Ia inserts into negatively charged membranes at low pH with a tertiary but little secondary structural change, *Biochemistry 32*, 2082−2089.
7. Zakharov, S. D., Rokitskaya, T. I., Shapovalov, V. L., Antonenko, Y. N., and Cramer, W. A. (2002) Tuning the membrane surface potential for efficient toxin import, *Proc. Natl. Acad. Sci. U.S.A. 99*, 8654−8659.
8. McLaughlin, S. (1989) The electrostatic properties of membranes, *Annu. Rev. Biophys. Biophys. Chem. 18*, 113−136.
9. Huster, D., Yao, X., Jakes, K., and Hong, M. (2002) Conformational changes of colicin Ia channel-forming domain upon membrane binding: A solid-state NMR study, *Biochim. Biophys. Acta 1561*, 159−170.
10. Hong, M., and Jakes, K. (1999) Selective and Extensive ^{13}C Labeling of a Membrane Protein for Solid-State NMR Investigation, *J. Biomol. NMR 14*, 71−74.
11. Hong, M. (1999) Determination of Multiple ϕ Torsion Angles in Solid Proteins by Selective and Extensive ^{13}C Labeling and Two-Dimensional Solid-State NMR, *J. Magn. Reson. 139*, 389−401.
12. Mayer, L. D., Hope, M. J., Cullis, P. R., and Janoff, A. S. (1985) Solute distributions and trapping efficiencies observed in freeze−thawed multilamellar vesicles, *Biochim. Biophys. Acta 817*, 193−196.
13. Hope, M. J., Bally, M. B., Webb, G., and Cullis, P. R. (1985) Production of large unilamellar vesicles by a rapid extrusion procedure. Characterization of size distribution, trapped volume, and ability to maintain a membrane potential, *Biochim. Biophys. Acta 812*, 55−65.
14. Smith, P. K., Krohn, R. I., Hermanson, G. T., Mallia, A. K., Gartner, F. H., Provenzano, M. D., Fujimoto, E. K., Goeke, N. M., Olson, B. J., and Klenk, D. C. (1985) Measurement of protein using bicinchoninic acid, *Anal. Biochem. 150*, 76−85.
15. Israelachvili, J. (1992) *Intermolecular and surface forces*, 2nd ed., Academic Press, San Diego.
16. Bennett, A. E., Rienstra, C. M., Auger, M., Lakshmi, K. V., and Griffin, R. G. (1995) Heteronuclear decoupling in rotating solids, *J. Chem. Phys. 103*, 6951−6958.
17. deAzevedo, E. R., Bonagamba, T. J., Hu, W., and Schmidt-Rohr, K. (1999) Centerband-only detection of exchange: Efficient analysis of dynamics in solids by NMR, *J. Am. Chem. Soc. 121*, 8411−8412.
18. deAzevedo, E. R., Bonagamba, T. J., Hu, W., and Schmidt-Rohr, K. (2000) Principle of centerband-only detection of the exchange and extension to a four-time CODEX, *J. Chem. Phys. 112*, 8988−9001.
19. Kolbert, A. C., De Groot, H. J. M., Levitt, M. H., Munowitz, M. G., Roberts, J. E., Harbison, G. S., Herzfeld, J., and Griffin, R. G. (1990) Two-dimensional dipolar-chemical shift NMR in rotating solids, in *Multinuclear Magnetic Resonance in Liquids and Solids-Chemical Applications* (Granger, P., and Harris, R. K., Eds.) pp 339−354, Kluwer Academic Publishers, Dordrecht, The Netherlands.
20. Rhim, W.-K., Elleman, D. D., and Vaughan, R. W. (1973) Analysis of multiple-pulse NMR in solids, *J. Chem. Phys. 59*, 3740−3749.
21. Van Rossum, B. J., De Groot, C. P., Ladizhansky, V., Vega, S., and De Groot, H. J. M. (2000) A Method for Measuring Heteronuclear (^{1}H−^{13}C) Distances in High-Speed MAS NMR, *J. Am. Chem. Soc. 122*, 3465−3472.
22. Hong, M., Yao, X. L., Jakes, K., and Huster, D. (2002) Investigation of molecular motions by Lee-Goldburg cross-polarization NMR spectroscopy, *J. Phys. Chem. B 106*, 7355−7364.
23. Kumashiro, K. K., Schmidt-Rohr, K., Murphy, O. J., Ouellette, K. L., Cramer, W. A., and Thompson, L. K. (1998) A novel tool for probing membrane protein structure: Solid-state NMR with proton spin diffusion and X-nucleus detection, *J. Am. Chem. Soc. 120*, 5043−5051.
24. Parker, M. W., Postma, J. P. M., Pattus, F., Tucker, A. D., and Tsernoglou, D. (1992) Refined structure of the pore-forming domain of colicin A at 2.4 Å resolution, *J. Mol. Biol. 224*, 639−657.
25. Lindeberg, M., Zakharov, S. D., and Cramer, W. A. (2000) Unfolding pathway of the colicin E1 channel protein on a membrane surface, *J. Mol. Biol. 295*, 679−692.

BI051540H